

# Comparative Studies of Multi-Photon Induced Emission by Pyridine-Based Small Molecular Probes in Biological Media: Selective Binding of Bioactive Molecules and In Vitro Imaging

Wanqing Wu,<sup>[a]</sup> Hoi-Kuan Kong,<sup>[b]</sup> Hongguang Li,<sup>[a]</sup> Yu-Man Ho,<sup>[c]</sup> Yuan Gao,<sup>[a]</sup> Jianhua Hao,<sup>[d]</sup> Margaret B. Murphy,<sup>\*[c]</sup> Michael Hon-Wah Lam,<sup>[c]</sup> Ka-Leung Wong,<sup>\*[b]</sup> and Chi-Sing Lee<sup>\*[a]</sup>

**Keywords:** Anions / Fluorescent probes / Imaging agents / Luminescence / Photochemistry

A new class of organic molecular probes (**1–3**) based on a 1,3-disubstituted diethynylbenzene core has been developed. Both **1** and **2** (with the esters of **1** replaced by diethylamides in **2**) show good linear and three-photon induced photophysical properties with two-photon absorption cross-sections ( $185\text{--}210\text{ cm}^4\text{ s photon}^{-1}\text{ molecule}^{-1}$ ) that are suitable for biological applications in live specimens. The propeller  $\pi$ -conjugated systems of **3** (a  $C_3$  analogue of **1**) shows threefold enhancement for the two-photon absorption cross-section ( $650\text{ cm}^4\text{ s photon}^{-1}\text{ molecule}^{-1}$ ). Solvatochromism was observed in the fluorescence spectra of all these molecular probes; in acidic medium (pH = 4–5) their fluorescence emis-

sions are slightly blueshifted with a threefold enhancement in intensity relative to those observed under basic conditions (pH = 10–11). In the fluorometric titration study against a variety of bioactive small molecules, only **2** shows strong binding affinity ( $\log K_B > 7$ ) towards citrates and bicarbonates with approximately 30 nm redshift. The in vitro emission spectra of **2** obtained show the same emission upon addition of anions to the solution. The results of these studies could provide new molecular-design strategies for two-photon absorption (TPA) chromophores and new materials for two-/multi-photon imaging in vitro.

## Introduction

Molecular imaging is used to detect, localize, and monitor critical molecular processes in cells, tissue, and living organisms, and requires highly sensitive instruments and contrast mechanisms.<sup>[1]</sup> The technique of cell immunolabeling and fluorescent imaging has been widely used in cell biology and clinical applications,<sup>[2]</sup> and this has helped to provide localization profiles and information about the quantity of the molecules of interest with no genetic modification required.<sup>[3]</sup> In general, there are many organic- and metal-based commercial molecular probes for in vitro and

even in vivo imaging; however, most have severe problems regarding their toxicity and the requirement for non-penetrative, ultraviolet emission excitation sources. Until the 2000s, fluorescence imaging mainly relied on UV excitation because of the lack of available fluorescent probes that were suitable for imaging in living cells using near-infrared (NIR) two-/multi-photon excitation. Recently, several two-/multi-photon absorption mechanisms have been established for organic,<sup>[4]</sup> organometallic,<sup>[5]</sup> and organic-lanthanide compounds.<sup>[6]</sup> Two-/multi-photon excitation allows molecules that typically absorb in the ultraviolet region to be excited by red or NIR light. The potential applications of multi-photon absorption processes (NIR excitation) shows promise in photonic and biomedical fields, and have recently stimulated the scientific community to develop and characterize new molecules with high multi-photon absorption profiles.<sup>[7]</sup> NIR excitation is one way to improve the quality of live-cell imaging, and the development of systems operating with NIR excitation and emission (700–900 nm) is a prime target, because NIR photons will not be absorbed by the cell, even in blood media. NIR photons can penetrate and be emitted from tissues without causing damage; moreover, the sharp emission profile gives clear imaging that can be differentiated from the usual biological autofluorescence background.<sup>[8]</sup>

[a] Laboratory of Chemical Genomics, School of Chemical Biology and Biotechnology, Peking University Shenzhen Graduate School, Shenzhen University Town, Xili, Shenzhen 518055, China  
E-mail: lizc@szpku.edu.cn

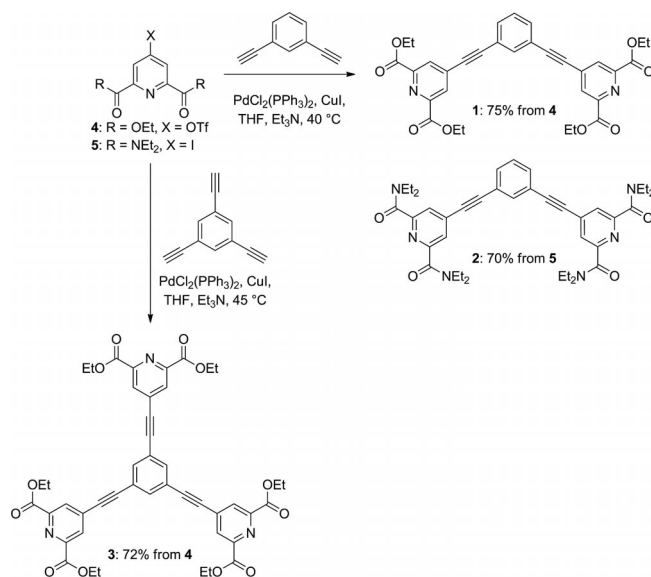
[b] Department of Chemistry, Hong Kong Baptist University, Kowloon Tong, Hong Kong SAR  
E-mail: klwong@hkbu.edu.hk

[c] Department of Biology and Chemistry, City University of Hong Kong, Kowloon Tong, TatChee Avenue, Hong Kong SAR  
E-mail: mbmurphy@cityu.edu.hk

[d] Department of Applied Physics, Hong Kong Polytechnic University, Hung Hum, Hong Kong SAR

Supporting information for this article is available on the WWW under <http://dx.doi.org/10.1002/ejoc.201100570>.

Organic compounds are generally more suitable for clinical use than metal complexes and nanomaterials, because they have no coordination instability problems and have more flexible properties. We are particularly interested in developing organic molecular probes with structures that are suitable for two/multi-photon in vitro and in vivo imaging through NIR excitation. Herein, we report the development of a new class of organic molecular probes **1–3**, based on the 1,3-disubstituted diethynylbenzene core (Scheme 1), with particular emphasis on their linear and two/multi-photon induced photo-physical properties, the dramatic change of their cell-permeable properties with slight structural modifications, and their use for in vitro imaging.



Scheme 1. Synthesis of organic molecular probes **1–3**.

## Results and Discussion

### Synthesis and Characterization of **1–3**

The organic molecular probes **1–3** were readily synthesized through a Sonogashira coupling strategy. As shown in Scheme 1, Pd-catalyzed cross-coupling of 1,3-diethynylbenzene with **4** (prepared through triflation of diethyl 4-hydroxypyridine-2,6-dicarboxylate<sup>[9]</sup> with Tf<sub>2</sub>O and pyridine) and **5**<sup>[10]</sup> afforded molecular probe **1** (75%) and **2** (95%), respectively. Sonogashira coupling between 1,3,5-triethynylbenzene and **4** under similar conditions provided molecular probe **3** in good yield. These compounds were characterized unambiguously by <sup>1</sup>H, <sup>13</sup>C NMR, and HRMS analyses.

### Linear Photophysical Properties of **1–3**

All the molecular probes (**1–3**) show intense absorption bands in the near-UV region. Molecular probes **1** and **2** in dimethyl sulfoxide (DMSO) have strong UV-absorption bands at  $\lambda$  ( $\epsilon$ ) = 270 (5.3), 310 (4.1), and 330 nm

(1.3 dm<sup>3</sup> mol<sup>-1</sup> cm<sup>-1</sup>), which are attributed to  $\pi$ - $\pi^*$  transitions. The absorption bands are similar to bands found in the excitation spectra in a solution of DMSO (10<sup>-5</sup> M) (Figure S1). The propeller  $\pi$ -conjugated system of **3** induces a significant redshift of the absorption bands (ca. 10 nm); in this case the bands are located at  $\lambda$  ( $\epsilon$ ) = 280 (6.1), 308 (4.6), 340 nm (1.7 dm<sup>3</sup> mol<sup>-1</sup> cm<sup>-1</sup>), and a new shoulder band is present at  $\lambda$  ( $\epsilon$ ) = 370 nm (0.5 dm<sup>3</sup> mol<sup>-1</sup> cm<sup>-1</sup>).

Molecular probes **1** and **2** gave very similar linear induced emission band shapes at 420 and 440 nm, respectively (Figure 1). The quantum yield of the emission bands of **1** and **2** in DMSO were 17 and 19%, respectively; these values were measured by using an integrating sphere with linear excitation at 350 nm. The quantum yield of **3** was slightly increased to 21% (Table 1).

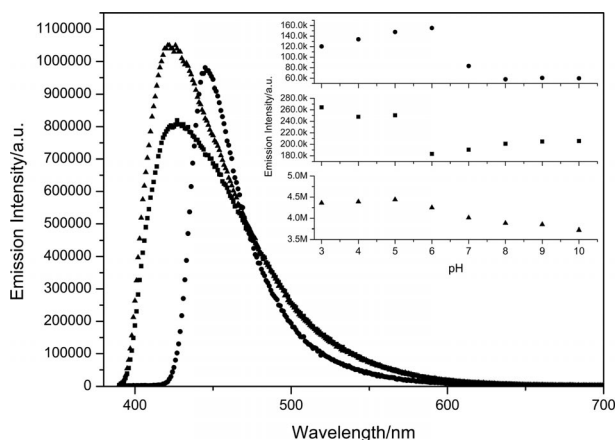


Figure 1. Emission spectra of **1** (squares), **2** (circles) and **3** (triangles) in DMSO (10  $\mu$ M,  $\lambda_{\text{ex}}$  = 350 nm). The inset shows the emission intensity of **1–3** plotted against the pH of the buffer solutions (pH = 3–10).

Table 1. Fluorescence quantum yields ( $\Phi$ ) and two-photon absorption cross sections ( $\sigma_2$ ) of **1–3** in DMSO (10  $\mu$ M).

	$\lambda_{\text{abs}}$ [nm] (log $\epsilon$ [dm <sup>3</sup> mol <sup>-1</sup> cm <sup>-1</sup> ])	$\Phi$ [%] <sup>[a]</sup>	$\sigma_2$ [GM] <sup>[b]</sup>
<b>1</b>	270 (5.32), 310 (4.15), 330 (1.31)	17	182
<b>2</b>	272 (5.3), 308 (4.0), 331 (1.28)	19	210
<b>3</b>	280 (6.1), 308 (4.6), 340 (1.7), 370 (0.5)	21	620

[a] Emission quantum yields of **1–3** ( $\lambda_{\text{em}}$  = 400–700 nm,  $\lambda_{\text{ex}}$  = 350 nm). [b] Two-photon absorption cross-section (GM = 10<sup>-50</sup> cm<sup>4</sup> s photon<sup>-1</sup> molecule<sup>-1</sup>,  $\lambda_{\text{ex}}$  = 750 nm).

Spectrophotometric analysis of **1–3** at various pH values revealed that their fluorescence emissions are pH-dependent. The relationship between the emission intensity and the pH is plotted in the inset of Figure 1. The emission spectra of **1–3** exhibited an intense peak at 422, 440, and 420 nm, respectively, in neutral pH, with bathochromic shifts to 430, 445, and 428 nm, respectively, at acidic pH. The emission intensity had a twofold decrease as the pH increased from 3 to 6 and became minimal beyond pH = 8.

### Two/Multi-Photon Induced Photophysical Properties of **1–3**

The emission maxima, band shape, and band width of **1–3** upon linear excitation can be reproduced by NIR exci-

tation (through multi-photon absorption). The linear and three-photon induced emission spectra of **1–3** are shown in Figure 1 (with UV excitation at 350 nm) and Figure 2 (excitation at 900 nm by a femtosecond laser), respectively. The linear absorption processes in **1–3** should be the same as the two- or three-photon absorption processes. Power-dependence experiments were performed to confirm the number of photons involved in the emission band under excitation at 900 nm (inset of Figure 2). In all cases, the output intensity of three-photon excited fluorescence (TPEF) was linearly dependent on the cube of the input laser intensity, thereby confirming three-photon absorption.

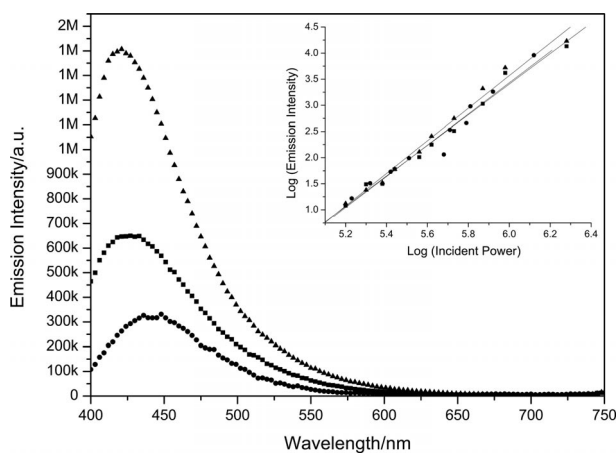


Figure 2. Three-photon induced emission spectra of **1** (squares), **2** (circles), and **3** (triangles) in DMSO. The inset shows the power-dependence experiments with **1–3** [ $10 \mu\text{M}$ ;  $\lambda_{\text{ex}} = 900 \text{ nm}$ ; **1**:  $\lambda_{\text{em}} = 420 \text{ nm}$  ( $n = 2.98$ ), **2**:  $\lambda_{\text{em}} = 440 \text{ nm}$  ( $n = 3.05$ ), **3**:  $\lambda_{\text{em}} = 425 \text{ nm}$  ( $n = 2.95$ )].

In general, the two-photon absorption cross-section of a material in solution is used to evaluate the strength of two-photon absorption and hence the possibility of two-photon induced visible imaging in vitro.<sup>[9]</sup> Thus, the two-photon absorption cross-section of **1** and **2** at 750 nm was measured and compared to that of Rhodamine 6G to establish their two-photon photophysical efficiency.<sup>[10]</sup> Molecular probe **1** (210 GM;  $\text{GM} = 10^{-50} \text{ cm}^4 \text{ s photon}^{-1} \text{ molecule}^{-1}$ ) demonstrated a higher two-photon absorption cross-section than **2** (185 GM). Both compounds were found to have much higher two-photon absorption values than the minimum suggested by Furuta et al. for biological applications ( $> 0.1 \text{ GM}$ ) in live specimens,<sup>[11]</sup> and the values were also higher than those of most organometallic compounds used for in vitro imaging (10–100 GM).<sup>[12]</sup> A difference (decrease) in the two-photon absorption cross-section could be induced by modifying the structure of the conjugated system (donor– $\pi$ –acceptor) in **2** by introducing a stronger electron-donating group. Significant enhancements of the TPA cross-section were observed in **3**, which is a derivative of compound **1** with an additional branch. The co-operative effects in the three branches of **3** significantly enhanced the two-photon absorption cross-section from 210 to 650 GM.

### Cation and Anion Binding Affinity and Selectivity

The binding properties of the organic molecular probes **1–3** in DMSO towards a variety of bioactive small molecules such as  $\text{Zn}^{2+}$ , citrate, and hydrogencarbonate was studied by using fluorometric titration. Changes in the emission spectral behavior were not very significant for **1** and **3**, but were still sufficient to allow the variation of the emission intensity with anion/cation concentration to be plotted and fitted to a 1:2 (analyte/probe) binding model. The affinity constants of **1–3** to several bioactive cations and anions were calculated and are summarized in Table 2. Adequate binding constants of **1** and **3** were observed for several anions/cations ( $\log K_{\text{B}} \approx 4$ , Table 2). Addition of  $\text{Zn}^{2+}$  reduced and redshifted (30 nm) the emission from approximately 430 to 460 nm (emission diminished obviously) for compound **3** (Figure 3).

Table 2. Affinity constants ( $\log K_{\text{B}}$ ) of the organic molecular probes for selected cations and anions (pH = 7.4, 0.1 M NaCl, 10  $\mu\text{M}$  compound **1–3**, 298 K,  $\lambda_{\text{ex}} = 350 \text{ nm}$ ).

	Citrate	$\text{KHCO}_3$	$\text{NaHCO}_3$	$\text{Na}_2\text{HPO}_4$	$\text{MgCl}_2$	KCl	NaCl	$\text{ZnCl}_2$
<b>1</b>	2.85	2.95	2.88	2.83	4.25	2.69	2.65	4.12
<b>2</b>	7.83	7.13	7.01	4.32	3.05	3.03	2.88	3.35
<b>3</b>	3.05	3.33	3.25	2.62	4.12	3.33	3.25	4.32

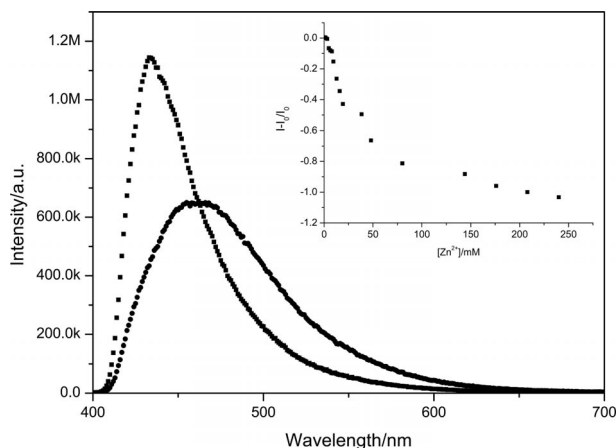


Figure 3. Responsive emission quenching of **3** (squares) in the presence of 250 mM of  $\text{ZnCl}_2$  (circles). The inset shows emission intensity ratio vs. amount of added zinc chloride (0.32  $\mu\text{M}$  to 240 mM), which was used to determine the apparent binding constant (pH = 7.4, 0.1 M NaCl, 10  $\mu\text{M}$  compound **3**, 298 K,  $\lambda_{\text{ex}} = 350 \text{ nm}$ ).

Significant optical changes were found for **2** upon the addition of anions, especially upon addition of citrate and bicarbonates. The partial positive charge of the amide nitrogen atoms of **2** could be responsible for the difference in anion-binding behavior compared with **1** and **3**. A relatively strong binding affinity of **2** was observed for hydrogen phosphate, citrate, and hydrogencarbonate (Table 2). Addition of citrate and bicarbonates led to a four-fold enhancement of emission, accompanied by a 30 nm (ca.  $3333 \text{ cm}^{-1}$ ) redshift, which allowed the emission intensity to be plotted as a function of added [citrate] or [hydrogencarbonate]; thus, an apparent 1:2 binding constant of

$10^{7.58(\pm 0.05)}$  for citrate, and  $10^{7.13(\pm 0.05)}$  for hydrogencarbonate were estimated for the citrate/hydrogencarbonate association (Figure 4).

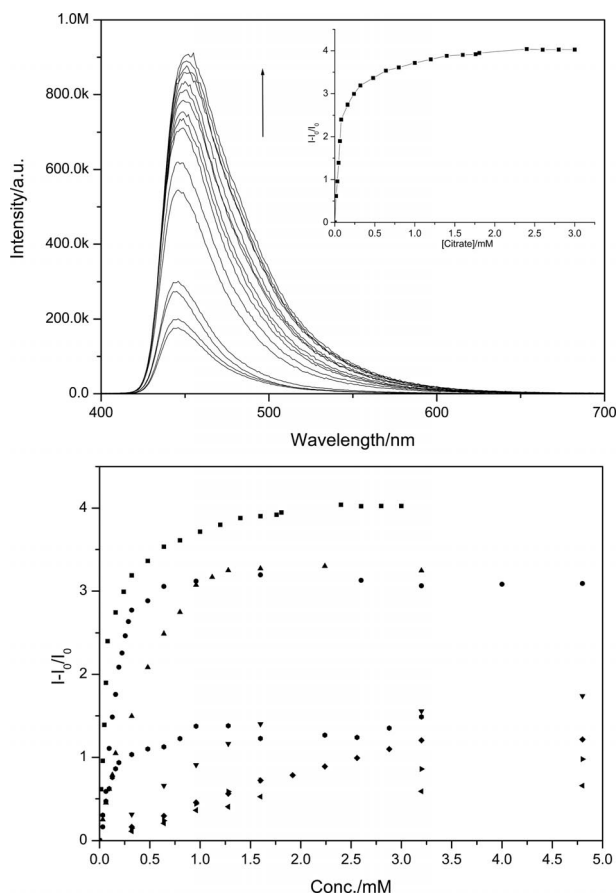


Figure 4. (Top) Emission spectra of **2** upon addition of sodium citrate (pH = 7.4, 0.1 M NaCl, 10  $\mu$ M compound **2**, 298 K,  $\lambda_{\text{ex}}$  = 350 nm), the inset shows the binding isotherm. (Bottom) Emission intensity ratio of compound **2** versus added analytes: sodium citrate (squares), sodium hydrogencarbonate (circles), potassium hydrogencarbonate (triangles-up), potassium chloride (triangles-down), magnesium chloride (diamonds), sodium chloride (triangles-left), zinc chloride (triangles-right), and sodium hydrogen phosphate (hexagons) to determine the apparent binding constants (pH = 7.4, 0.1 M NaCl, 10  $\mu$ M compound **2**, 298 K,  $\lambda_{\text{ex}}$  = 350 nm).

### In Vitro Imaging and Cytotoxicity Studies

The performance of **1–3** in vitro was evaluated with a variety of assays including linear, two/multi-photon confocal imaging, and toxicity tests (MTT assay and IC<sub>50</sub> determination). For in vitro imaging, molecular probes **1–3** were added to the same amounts of two carcinoma cell lines (Human cervical carcinoma HeLa and Human lung carcinoma A549), and the samples were examined at various points of time. For **1** and **3**, no emission could be observed in the cells; only a strong bluish green emission could be obtained from the tissue culture medium (Figure S2). However, molecular probe **2** demonstrated strong green emissions in the in vitro imaging (Figure 5); 1 h after dosage, weak emission could be observed under UV and NIR exci-

tation that was localized within the cytoplasm of the cells (Figure 5a). After 6 and 12 h of incubation, more than 90% of cells emitted under NIR excitation (Figure 5c and Figure 5d, respectively). The most interesting finding for our molecular probes was their NIR excited induced visible photophysical properties. The in vitro imaging and emission spectra of **2** were recorded and are shown in Figure 6. After 3 h of dosage time, strong green emission in the 400–650 nm region could be observed in the cytoplasm of HeLa cells under excitation at 900 nm (50 mW). A lambda scan of a confocal microscope (resolution 6 nm) was recorded that showed green emission bands inside the cytoplasm of HeLa cells. The emission band shape and maximum shown in Figure 6 were the same as the emission spectra shown in Figure 4; a 30 nm redshift was obtained that indicated that the molecular probe was bonded to the anions, and that a strong three-photon induced emission with a fingerprint redshifted emission was established. This experiment showed that, in the presence of anions, molecular probe **2** can reproduce the same emission spectra in solution (Figure 4) and in vitro (Figure 6) under either linear or two-photon excitation.

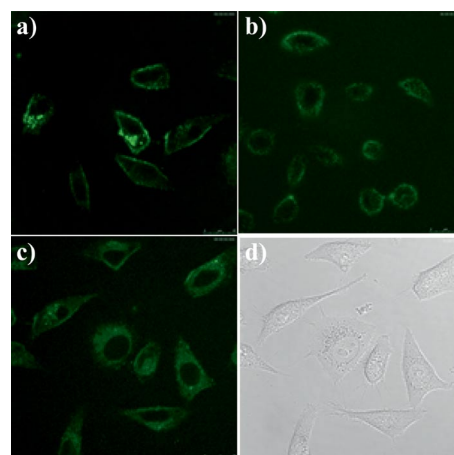


Figure 5. In vitro cytoplasmic staining microscopy with **2** (50  $\mu$ M,  $\lambda_{\text{ex}}$  = 900 nm,  $\lambda_{\text{em}}$  = 450–750 nm) in A549 after (a) 1 h, (b) 6 h, and (c) 12 h. (d) Bright-field image of panel (c).

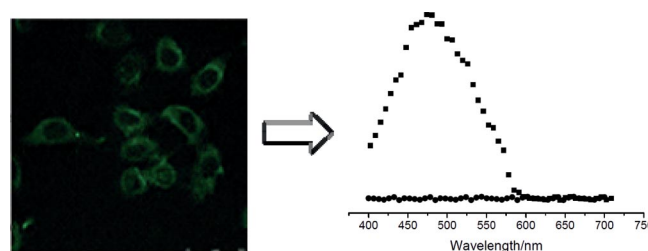


Figure 6. (Left) Multi-photon (NIR) induced in vitro imaging of HeLa cells after 12 h of incubation with **2**. (Right) In vitro emission spectra of the two regions in the visible and NIR region obtained by using the  $\lambda$  scan of a Leica SP5 laser fluorescent microscope (resolution ca. 6 nm,  $\lambda_{\text{ex}}$  = 900 nm); (squares) channel 1, green emission in HeLa cells; (circles) channel 2, background.

We extended the application of these three organic molecules as potential citrate or hydrogencarbonate probes for in vitro imaging. Toxicity tests with the three compounds were performed, and no evidence of cytotoxicity on HeLa cells was found upon exposure to **1–3** (50  $\mu\text{M}$ ) for 24 h (Figure 7). MTT assays on cells exposed to 50  $\mu\text{M}$  **1–3** (as high as 20 times the dosage concentration required for in vitro imaging) for prolonged periods revealed no significant decrease in the number of viable cells. In addition, the non-toxic  $\text{IC}_{50}$  values (ca. 22 mM, ca. 25 mM and ca. 18 mM for **1–3**, respectively) of the complexes in HeLa cells were found to distribute inside the cytoplasm and can be further developed as specific imaging probes with connection to vectors such as peptides. It is worth noting that the molecular probes were mostly distributed inside the cytoplasm and could be further developed as specific imaging probes with connection to vectors such as peptides.

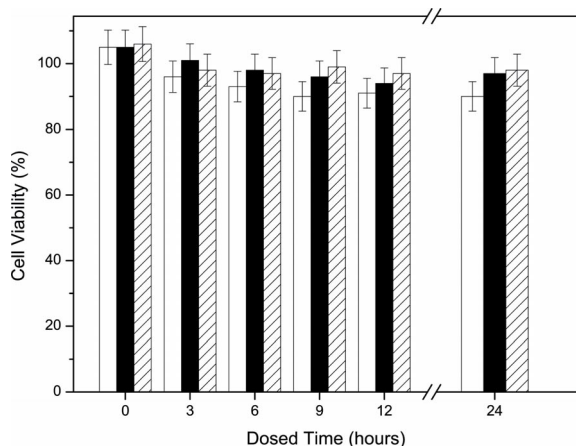


Figure 7. MTT assay for cytotoxicity of **1** (white bars), **2** (black bars) and **3** (hatched bars) in HeLa cells.

## Conclusions

We have developed a new class of organic molecular probes **1–3** based on the 1,3-disubstituted diethynylbenzene core. Both **1** and **2** (with the esters of **1** replaced by diethylamides in **2**) show good linear and three-photon induced photophysical properties with two-photon absorption cross-section (185–210 GM) that are suitable for biological applications in live specimens. Molecular probe **3** has an additional  $\pi$ -conjugated branch forming a  $C_3$  analogue of **1**. The propeller  $\pi$ -conjugated system of **3** shows a co-operative effect that induces a threefold enhancement of the two-photon absorption cross-section compared with **1** and **2**, which contain only two  $\pi$ -conjugated systems. More interestingly, molecular probe **2**, with the partial positive charged amides, shows specific binding to anions, particularly citrate and hydrogencarbonate, exhibits more cell permeability, and is capable of producing emission spectra in vitro upon excitation with NIR irradiation within the “biological window” (700–1000 nm) in cellular studies. These results indicate the possibility of structurally modifying the

organic molecules to improve cell permeability. The results also confirm NIR induced emission occurs after two/multi-photon absorption, which has potential applications both in vitro and in vivo, especially for **2**. These findings can be applied in the design of new materials that make use of highly penetrating NIR excitation sources and more target-specific emissions, and should advance investigations on human cells.

## Experimental Section

### Synthesis of Organic Molecular Probes **1–3**

**General Information:** All air- and water-sensitive reactions were carried out under nitrogen with anhydrous solvents under anhydrous conditions, unless otherwise noted. All chemicals were purchased and used without further purification. Anhydrous THF was distilled from sodium/benzophenone, and dichloromethane was distilled from calcium hydride. Yields refer to chromatographically pure products, unless otherwise stated. NMR spectra were recorded with either a Bruker Avance 300 ( $^1\text{H}$ : 300 MHz;  $^{13}\text{C}$ : 75.5 MHz) or a Bruker Avance 500 ( $^1\text{H}$ : 500 MHz;  $^{13}\text{C}$ : 125.8 MHz) spectrometer. The following abbreviations were used for multiplicities: s = singlet, d = doublet, t = triplet, q = quartet, m = multiplet, br. = broad. High-resolution mass spectra were obtained with an Applied Biosystems (ABI) Q-Star Elite MALDI-TOF mass spectrometer.

**Diethyl 4-(Trifluoromethylsulfonyloxy)pyridine-2,6-dicarboxylate (**4**):** To a solution of diethyl 4-hydroxypyridine-2,6-dicarboxylate<sup>[13]</sup> (0.14 g, 0.59 mmol) in  $\text{CH}_2\text{Cl}_2$  (5 mL) at  $-78^\circ\text{C}$ , were added pyridine (0.30 mL, 3.56 mmol) and  $\text{Ti}_2\text{O}$  (0.30 mL, 1.78 mmol). After stirring at  $-78^\circ\text{C}$  for 2 h, the reaction was quenched with water. The aqueous phase was extracted with ethyl acetate (3 $\times$ ), and the combined extracts were washed with brine, dried with  $\text{MgSO}_4$ , filtered, and concentrated under reduced pressure. Silica gel flash column chromatography (hexanes/ethyl acetate = 5:1 to 3:1) of the residue gave the product as a white solid (0.18 g, 80%).  $^1\text{H}$  NMR (500 MHz,  $\text{CDCl}_3$ ):  $\delta$  = 8.17 (s, 2 H), 4.53 (q,  $J$  = 7.2 Hz, 4 H), 1.48 (t,  $J$  = 7.2 Hz, 6 H) ppm.  $^{13}\text{C}$  NMR (125 MHz,  $\text{CDCl}_3$ ):  $\delta$  = 163.1, 157.7, 151.8, 120.2, 117.4, 63.0, 14.2 ppm. HRMS (ESI): calcd. for  $\text{C}_{12}\text{H}_{13}\text{NO}_7\text{F}_3\text{S}$  [ $\text{M} + \text{H}$ ] $^+$  372.0365; found 372.0362.

**Tetraethyl 4,4'-[1,3-Phenylenebis(ethyne-2,1-diyl)]dipyridine-2,6-dicarboxylate (**1**):** To a solution of 1,3-diethynylbenzene (0.20 mL, 1.49 mmol), **4** (1.0 g, 2.70 mmol), and CuI (26 mg, 0.135 mmol) in THF (10 mL) was added  $\text{Et}_3\text{N}$  (10 mL), followed by  $[\text{PdCl}_2(\text{PPh}_3)_2]$  (28 mg, 0.041 mmol). After stirring at  $40^\circ\text{C}$  overnight, the reaction was quenched with saturated aqueous  $\text{NH}_4\text{Cl}$ . The aqueous phase was extracted with diethyl ether (3 $\times$ ), and the combined extracts were washed with brine, dried with  $\text{Na}_2\text{SO}_4$ , filtered, and concentrated under reduced pressure. Silica gel flash column chromatography (dichloromethane/methanol = 100:1 to 50:1) of the residue gave the product as a pale-yellow solid (0.58 g, 75%). M.p. 116–124  $^\circ\text{C}$ .  $^1\text{H}$  NMR (500 MHz,  $\text{CDCl}_3$ ):  $\delta$  = 8.32 (m, 4 H), 7.77 (m, 1 H), 7.58 (m, 2 H), 7.42 (m, 1 H), 4.50 (q,  $J$  = 7.1 Hz, 8 H), 1.46 (t,  $J$  = 7.1 Hz, 12 H) ppm.  $^{13}\text{C}$  NMR (125 MHz,  $\text{CDCl}_3$ ):  $\delta$  = 167.3, 149.2, 135.9, 135.5, 133.9, 133.8, 133.7, 133.1, 132.8, 129.5, 129.2, 129.0, 122.5, 95.0, 86.6, 62.6, 14.3 ppm. HRMS (ESI): calcd. for  $\text{C}_{32}\text{H}_{29}\text{N}_2\text{O}_8$  [ $\text{M} + \text{H}$ ] $^+$  569.1918; found 569.1913.

**4,4'-[1,3-Phenylenebis(ethyne-2,1-diyl)]bis( $N^2,N^2,N^6,N^6$ -tetraethylpyridine-2,6-dicarboxamide) (**2**):** To a solution of 1,3-diethynylbenzene (30  $\mu\text{L}$ , 0.21 mmol),  $N^2,N^2,N^6,N^6$ -tetraethyl-4-iodopyridine-2,6-dicarboxamide<sup>[14]</sup> (0.16 g, 0.40 mmol), and CuI (13 mg,

0.065 mmol) in THF (5 mL), was added Et<sub>3</sub>N (5 mL), followed by [PdCl<sub>2</sub>(PPh<sub>3</sub>)<sub>2</sub>] (23 mg, 0.03 mmol). After stirring at 40 °C overnight, the reaction was quenched with saturated aqueous NH<sub>4</sub>Cl. The aqueous phase was extracted with diethyl ether (3 ×), and the combined extracts were washed with brine, dried with Na<sub>2</sub>SO<sub>4</sub>, filtered, and concentrated under reduced pressure. Silica gel flash column chromatography (dichloromethane/methanol = 100:1 to 50:1) of the residue gave the product as a pale-yellow solid (95 mg, 70%). M.p. 83–84 °C. <sup>1</sup>H NMR (500 MHz, CDCl<sub>3</sub>): δ = 7.70 (m, 5 H), 7.54 (m, 2 H), 7.38 (m, 1 H), 3.56 (q, *J* = 7.1 Hz, 8 H), 3.35 (q, *J* = 7.1 Hz, 8 H), 1.26 (t, *J* = 7.1 Hz, 12 H), 1.15 (t, *J* = 7.1 Hz, 12 H) ppm. <sup>13</sup>C NMR (125 MHz, CDCl<sub>3</sub>): δ = 167.6, 154.1, 135.3, 133.4, 132.9, 129.0, 125.5, 122.7, 94.2, 87.0, 43.4, 40.4, 14.4, 12.9 ppm. HRMS (ESI): calcd. for C<sub>40</sub>H<sub>49</sub>N<sub>6</sub>O<sub>4</sub> [M + H]<sup>+</sup> 677.3810; found 677.3814.

**Hexaethyl 4,4',4''-[Benzene-1,3,5-triyltris(ethyne-2,1-diyl)]tris(pyridine-2,6-dicarboxylate) (3):** To a solution of 1,3,5-triethynylbenzene (0.33 g, 2.16 mmol), **4** (2.0 g, 5.41 mmol), and CuI (34 mg, 0.18 mmol) in THF (10 mL), was added Et<sub>3</sub>N (10 mL), followed by [PdCl<sub>2</sub>(PPh<sub>3</sub>)<sub>2</sub>] (38 mg, 0.054 mmol). After stirring at 45 °C overnight, the reaction was quenched with saturated aqueous NH<sub>4</sub>Cl. The aqueous phase was extracted with diethyl ether (3 ×), and the combined extracts were washed with brine, dried with Na<sub>2</sub>SO<sub>4</sub>, filtered, and concentrated under reduced pressure. Silica gel flash column chromatography (dichloromethane/methanol = 100:1 to 50:1) of the residue gave the product as a pale-yellow solid (1.05 g, 72%). M.p. 195–200 °C (dec). <sup>1</sup>H NMR (300 MHz, CDCl<sub>3</sub>): δ = 8.36 (s, 6 H), 7.83 (s, 3 H), 4.52 (q, *J* = 7.1 Hz, 12 H), 1.48 (t, *J* = 7.1 Hz, 18 H) ppm. <sup>13</sup>C NMR (75.5 MHz, CDCl<sub>3</sub>): δ = 164.2, 149.2, 136.0, 133.4, 129.6, 123.2, 93.6, 87.4, 62.8, 14.4 ppm. HRMS (ESI): calcd. for C<sub>45</sub>H<sub>40</sub>N<sub>3</sub>O<sub>12</sub> [M + H]<sup>+</sup> 814.2607; found 814.2607.

**Spectroscopic and Photophysical Measurements:** UV/Vis absorption spectra in the spectral range 200–1100 nm were recorded with an HP UV-8453 spectrophotometer. Single-photon luminescence spectra were recorded with an Edinburgh Instrument FLS920 Combined Fluorescence Lifetime and Steady-state spectrophotometer that was equipped with a red-sensitive single-photon counting photomultiplier in a Peltier Cooled Housing. The spectra were corrected for detector response and stray background light phosphorescence. The quantum yields of compounds **1–3** were measured with a demountable 142 mm (inner) diameter barium sulfide coated integrating sphere supplied with two access ports. For multi-photon experiments, the 900 nm pump source was from a femtosecond mode locked Ti:Sapphire laser system (output beam ca. 150 fs duration and 1 kHz repetition rate). The lasers were focused to a spot size of approximately 50 μm by an *f* = 10 cm lens onto the sample. The emitting light was collected with a backscattering configuration into a 0.5 m spectrograph and detected by a liquid nitrogen cooled CCD detector. A power meter was used to monitor the uniform excitation. The theoretical framework and experimental protocol for the two-photon cross-section measurement have been outlined by Webb and Xu.<sup>[15]</sup> In this approach, the two-photon excitation (TPE) ratios of the reference and sample systems are given by:

$$\frac{\sigma_2^S \cdot \phi^S}{\sigma_2^R \cdot \phi^R} = \frac{C_R \cdot n_S \cdot F^S(\lambda)}{C_S \cdot n_R \cdot F^R(\lambda)}$$

where  $\phi$  is the quantum yield,  $C$  is the concentration,  $n$  is the refractive index, and  $F(\lambda)$  is the integrated photoluminescent spectrum. In our measurements, we have ensured that the excitation flux and the excitation wavelengths are the same for both the sample and

the reference. The two-photon absorption cross-section  $\sigma_2$  of **1–3** was determined by using Rhodamine 6G as a reference. For spectrofluorometric titrations, all the solvents used were of analytical grade, and the water used was purified by double distillation. Measurements were taken after equilibrium was attained, and the emission of the compound was monitored. Luminescent responses in terms of  $I_0/(I - I_0)$  were plotted as a function of analyte concentration. For the determination of binding strengths of the various analyte adducts, a series of analyte solutions of known concentrations were mixed with the anion solutions at various concentrations. The titration curve was then fitted either with the 1:1, 1:2, or 1:3 Benesi–Hildebrand equations to establish which type of donor–acceptor interaction existed.<sup>[16]</sup>

**Microscopy Imaging:** To study the behavior of compounds **1–3** in vitro, experiments were conducted by using a commercial multi-photon confocal microscope. For two-photon imaging in vitro, the cells were imaged in a tissue culture chamber (5% CO<sub>2</sub>, 37 °C) by using a Leica SP5 (upright configuration) confocal microscope equipped with a femtosecond-pulsed Ti:Sapphire laser (Libra II, Coherent). The excitation beam was produced by the femtosecond laser, which was tuneable in the range 680–1050 nm ( $\lambda_{\text{ex}}$  = 900 nm, ca. 5 mW), and focused on coverslip-adherent cells by using a 40 × oil-immersion objective.

**Cell Culture:** Human lung carcinoma A549 cells were purchased from the American Type Culture Collection (ATCC) (#CCL-185, ATCC, Manassas, VA, USA). Cells were cultured in Ham's F12K medium with L-glutamine and phenol red (N3520, Sigma, St. Louis, MO, USA) supplemented with 10% fetal bovine serum at 37 °C and 5% CO<sub>2</sub>. Cells were passaged every 3–5 d. Human cervical carcinoma (HeLa) cells were maintained in an RPMI 1640 medium supplemented with 10% fetal bovine serum (FBS) and 1% penicillin and streptomycin in 5% CO<sub>2</sub>. The MTT viability assay was performed as reported previously.<sup>[17]</sup> Briefly, three thousand HeLa cells were seeded in 96-well plates 24 h prior to exposure to compounds **1–3** or DMSO as control. After various exposure time points, 20 μL of MTT [3-(4,5-dimethylthiazol-2-yl)-2,5-diphenyltetrazolium bromide] solution (5 mg/mL) was added to the culture medium in each well and incubated at 37 °C for 5 h. The media was removed, 200 μL of DMSO solubilizing reagent was added, and incubation was continued for a further 1 h to dissolve the formazan crystals. The absorbance was measured at 570 nm with a Labsystem Multiskan microplate reader (Merck Eurolab, Switzerland). MTT assays were conducted in triplicate wells, and repeated twice. Each data point represents the ratio of mean values between the compounds versus the DMSO control.

**Supporting Information** (see footnote on the first page of this article): UV/Vis absorption, excitation spectra, in vitro imaging of **1** and **3**, <sup>1</sup>H NMR and <sup>13</sup>C NMR spectra of molecular probes **1–3**.

## Acknowledgments

This work was funded by grants from the Peking University Shenzhen Graduate School, the Hong Kong Research Grants Council, the City University of Hong Kong, and the Hong Kong Baptist University (FRG1/10-11/037).

- [1] N. A. Campbell, *Biology*, 4th ed., Benjamin/Cummings Publishing, Menlo Park, California, 1996.
- [2] S. Jakobs, *Biochim. Biophys. Acta* **2006**, *1763*, 561–575.
- [3] www.invitrogen.com and the references cited therein.

- [4] a) S. Feng, Y. K. Kim, S. Yang, T.-T. Chang, *Chem. Commun.* **2010**, 46, 436–438; b) C.-H. Chui, Q. Wang, W.-C. Chow, M. C.-W. Yuen, K.-L. Wong, W.-M. Kwok, G. Y.-M. Cheng, R. S.-M. Wong, S.-W. Tong, K.-W. Chan, F.-Y. Lau, P. B.-S. Lai, K.-H. Lam, E. Fabbri, X.-M. Tao, R. Gambari, W.-Y. Wong, *Chem. Commun.* **2010**, 46, 3538–3540; c) Y.-T. Shen, C.-H. Li, K.-C. Chang, S.-Y. Chin, H.-A. Lin, Y.-M. Liu, C.-Y. Hung, H.-F. Hsu, S.-S. Sun, *Langmuir* **2009**, 25, 8714–8722; d) C. Barsu, R. Fortrie, K. Nowika, P. L. Baldeck, J.-C. Vial, A. Barsella, A. Fort, M. Hissler, Y. Bretonnière, O. Maury, C. Andraud, *Chem. Commun.* **2006**, 4744–4746.
- [5] C.-K. Koo, P. L. K.-Y. So, P. K.-L. Wong, P. Y.-W. Lam, M. H.-W. Lam, K.-W. Cheah, *Chem. Eur. J.* **2010**, 16, 3942–3950.
- [6] a) J. C. Bünzli, *Chem. Rev.* **2010**, 110, 2729–2755; b) G.-L. Law, R. Pal, L. O. Palsson, D. Parker, K.-L. Wong, *Chem. Commun.* **2009**, 7321; c) G.-L. Law, K.-L. Wong, C. W.-Y. Man, S.-W. Tsao, W.-T. Wong, *J. Biophotonics* **2009**, 2, 718–724.
- [7] a) G. S. He, L.-S. Tan, Q. Zheng, P. N. Prasad, *Chem. Rev.* **2008**, 108, 1245–1330; b) G.-L. Law, K.-L. Wong, W.-M. Kwok, P. A. Tanner, W.-T. Wong, *J. Phys. Chem. B* **2007**, 111, 10858–10861.
- [8] J. V. Frangioni, *Curr. Opin. Chem. Biol.* **2003**, 7, 626–634.
- [9] a) R. M. Williams, W. R. Zipfel, W. W. Webb, *Curr. Opin. Chem. Biol.* **2001**, 5, 603–608; b) G. Piszczek, I. Gryczynski, B. P. Maliwal, J. R. Lakowicz, *J. Fluoresc.* **2002**, 12, 15–17.
- [10] S. Mathai, D. K. Bird, S. S. Stylli, T. A. Smith, K. P. Ghiggino, *Photochem. Photobiol. Sci.* **2007**, 9, 1019–1026.
- [11] T. Furuta, S. S.-S. Wang, J.-L. Dantzker, T.-M. Dore, W.-J. Bybee, E.-M. Callaway, W. Denk, R. Y. Tsien, *Proc. Natl. Acad. Sci. USA* **1999**, 96, 1193–1200.
- [12] K. K.-W. Lo, M.-W. Louie, K. Y. Zhang, *Coord. Chem. Rev.* **2010**, 254, 2603–2622.
- [13] P. Froidevaux, J. M. Harrowfield, A. N. Sobolev, *Inorg. Chem.* **2000**, 39, 4678–4687.
- [14] A. Picot, C. Feuvrie, C. Barsu, F. Malvotti, B. L. Guennic, H. L. Bozec, C. Andraud, L. Toupet, O. Maury, *Tetrahedron* **2008**, 64, 399–411.
- [15] X. Xu, W. W. Webb, *J. Opt. Soc. Am. B* **1996**, 13, 481–491.
- [16] O. Kahn, *Acc. Chem. Res.* **2000**, 33, 647–657.
- [17] A. P. Wilson, *Cytotoxicity and Viability Assays in Animal Cell Culture: A Practical Approach*, 3rd ed. (Ed.: J. R. W. Masters) Oxford University Press, Oxford, **2000**, p. 1.

Received: April 23, 2011

Published Online: July 26, 2011